University of Massachusetts Amherst

From the SelectedWorks of Alfred Crosby

December 26, 2007

Friction of Soft Elastomeric Surfaces with a Defect

Charles J. Rand
Alfred Crosby, *University of Massachusetts - Amherst*

Available at: https://works.bepress.com/alfred_crosby/20/

AIP Journal of Applied Physics

Friction of soft elastomeric wrinkled surfaces

Charles J. Rand and Alfred J. Crosby

Citation: Journal of Applied Physics **106**, 064913 (2009); doi: 10.1063/1.3226074
View online: http://dx.doi.org/10.1063/1.3226074
View Table of Contents: http://scitation.aip.org/content/aip/journal/jap/106/6?ver=pdfcov
Published by the AIP Publishing

Advertisement:

[This article is copyrighted as indicated in the abstract. Reuse of AIP content is subject to the terms at: http://scitation.aip.org/termsconditions. Downloaded to] IP: 128.119.168.228 On: Mon, 28 Oct 2013 15:50:39

Friction of soft elastomeric wrinkled surfaces

Charles J. Rand and Alfred J. Crosby[a)]
Department of Polymer Science and Engineering, University of Massachusetts, Amherst, Massachusetts 01003, USA

(Received 7 July 2009; accepted 19 August 2009; published online 25 September 2009)

We evaluate the sliding of a rigid spherical lens over a surface-wrinkled, elastomeric substrate. Sliding is conducted both parallel and perpendicular to the aligned surface wrinkles, and the sliding force is compared to the required sliding forces on nonwrinkled surfaces. We evaluate the effects of wrinkle dimensions and applied normal force on the sliding resistance. A simple Bowden–Tabor friction model can describe the dependence of the sliding force on normal load, with different coefficients of friction associated with the nonwrinkled and wrinkled surfaces both perpendicular and parallel. The aspect ratio of the wrinkles has a secondary effect on the sliding force. We associate the changes in friction to changes in the tangential stiffness and fracture angle caused by the surface wrinkles. © *2009 American Institute of Physics*. [doi:10.1063/1.3226074]

I. INTRODUCTION

Taking a cue from nature, scientists have looked to topographical patterns to tune the interfacial adhesion and friction of soft elastomeric surfaces. While a large fraction of the published work has focused on biomimetic structures for enhanced adhesion,[1–8] a growing emphasis has been placed on topographic structures, such as high aspect ratio fibrils and mushroom-shaped structures, for the tuning of interfacial friction.[9,10] Although most efforts for surface patterning have relied upon lithographically derived methods, recent work has suggested that surface wrinkling of a soft substrate can provide a robust mechanism for the development of structures that can efficiently alter interfacial properties.[11] Building on this, we present experimental results focused on the effect of surface wrinkle structures on sliding friction and discuss the advantages of using this simple patterning procedure as a systematic tool for tuning the friction of polymer surfaces.

We evaluate a rigid lens sliding over flat and surface-wrinkled soft elastomeric surfaces. In the absence of wrinkles, sliding proceeds through a Schallamach wave mechanism.[12] The addition of wrinkles changes the frictional mechanism to either a stick-slip or true-sliding mechanism, disrupting the formation of Schallamach waves in almost all of the samples. We evaluate sliding friction as a function of wrinkle periodicity, wrinkle amplitude, applied normal load, and sliding direction relative to wrinkle orientation.

II. EXPERIMENTAL

Wrinkled surfaces were created using the following process. Crosslinked polydimethylsiloxane (PDMS) (Dow Corning's Sylgard® 184) samples were prepared using three different crosslinker to prepolymer ratios 1 to 10, 1 to 15, and 1 to 20. Samples were cast as films 1 mm thick, and dog bone shaped specimens were cut from the films. The samples were then subjected to uniaxially applied mechanical strain equal to 30% and exposed to ultraviolet light in the presence of ozone (UVO) for durations of 45, 60, 75, and 90 min. This UVO process converts the surface of the PDMS into a silicalike layer (SiO_x).[13–15] After UVO processing, the mechanical strain was released to create samples with aligned wrinkles of varying periodicity and amplitude as controlled by the UVO process time and the crosslinker to prepolymer ratio of the PDMS.[16] To focus on the effect of wrinkle topography and eliminate the effect of different material properties used to achieve various wrinkle parameters, molds were templated from wrinkled surfaces using Norland Optical Adhesive 60 (Edmunds Optics), a photocurable optical adhesive. The molds of the various wrinkled samples were used to cast fresh films of crosslinked PDMS with one crosslinker to prepolymer ratio (1 to 10). These wrinkled PDMS surfaces were then swollen in hexane for two days and dried to minimize the number of free siloxane chains at the surface. A schematic of the production of uniaxially aligned PDMS wrinkled surfaces is shown in Fig. 1. Molds were characterized using stylus profilometry to quantify the wrinkle periodicity and wrinkle amplitude. Crosslinked PDMS films of thickness 1 mm with crosslinker to prepolymer ratio of 1 to 10 were prepared without wrinkled surfaces to serve as a control.

Using the procedure outlined above, we produced a library of surface-wrinkled samples with different aspect ratios or h/λ, as shown in Fig. 2. Figure 2 shows that the

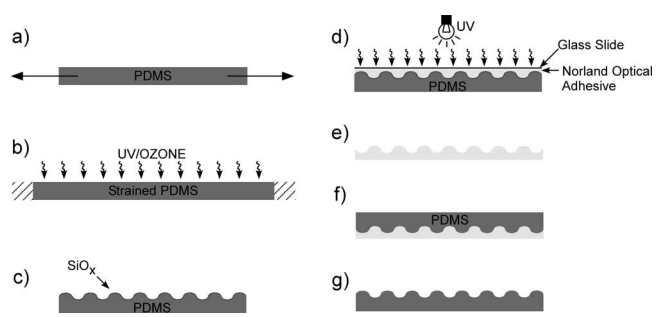

FIG. 1. Process for fabricating aligned wrinkle surfaces, free of residual stresses.

[a)]Electronic mail: crosby@mail.pse.umass.edu.

 © 2009 American Institute of Physics

[This article is copyrighted as indicated in the abstract. Reuse of AIP content is subject to the terms at: http://scitation.aip.org/termsconditions. Downloaded to] IP: 128.119.168.228 On: Mon, 28 Oct 2013 15:50:39

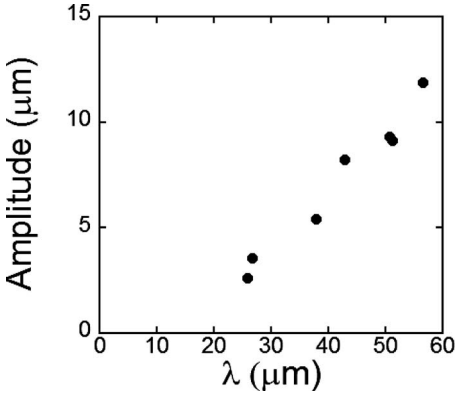

FIG. 2. Amplitude vs buckle periodicity (λ).

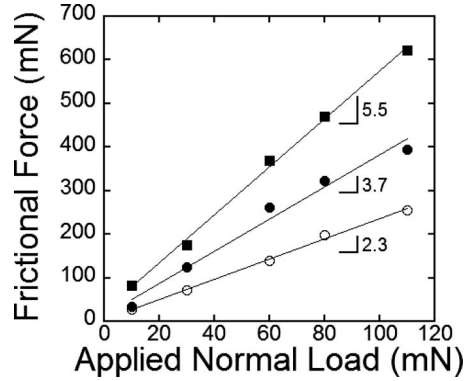

FIG. 4. Frictional force vs normal load (■—flat surface, ●—sliding parallel to the wrinkles, and ○—sliding perpendicular to the wrinkles).

amplitude increases linearly with the buckle periodicity of the wrinkles. The linear scaling relationship of amplitude to buckle periodicity at a constant compressive strain has been described previously by Cerda and Mahadevan.[17]

Specimen surfaces were subjected to frictional experiments using a custom built instrument previously described.[18] In brief, a polished fused silica glass hemisphere (radius of curvature $R=5$ mm) was translated in contact with PDMS surfaces, both parallel and perpendicular to the wrinkle alignment direction, under a fixed normal load, P. Lateral sliding force, sliding distance, and images of the interfacial area were recorded continuously during sliding. For experiments concerning the effect of wrinkle dimensions, the wrinkle amplitude (h) and periodicity (λ) were varied (Fig. 2) and the normal load remained constant $P\sim 23$ mN. For nonwrinkled surfaces and a wrinkled surface of $h=3.6$ μm and $\lambda=26.6$ μm, the normal loads applied during sliding were 10, 30, 60, 80, and 110 mN. The lateral sliding velocity (v) was fixed at 5 μm/s for all experiments.

III. RESULTS

Representative data showing the sliding force as a function of sliding position is shown in Fig. 3. Oscillations in the sliding force for the flat sample are associated with the formation and attachment of Schallamach waves, as discussed in previous papers.[18,19] In the wrinkled sample, for sliding both parallel and perpendicular to the wrinkles, the frictional force does not oscillate and maintains a constant value, which is associated with a true-sliding frictional mechanism.

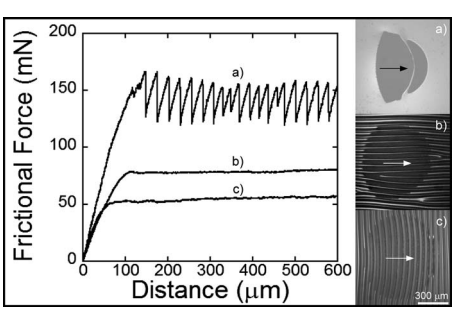

FIG. 3. Representative force-displacement curves and sliding images for flat and wrinkled surfaces. (a) Sliding on a smooth surface, (b) sliding parallel to the wrinkles, and (c) sliding perpendicular to the wrinkles. (Arrows indicate direction of sliding.)

It should be noted that from the sliding images of the wrinkled surface, the critical load required to collapse the wrinkles has not been reached and hence the valleys of the wrinkles are not in contact with the slider.[20] The critical normal load per surface area for collapsing surface wrinkles under nonsliding conditions scales with the wrinkle amplitude, modulus of the wrinkles and inversely as the buckle periodicity.[21] For sliding both parallel and perpendicular to the wrinkles, a decrease in the sliding frictional force compared to the flat surface is observed, with a greater decrease observed for sliding perpendicular to the wrinkles.

A load dependence study was conducted on surfaces with wrinkles with an aspect ratio of 0.135. Sliding friction forces were measured for sliding parallel and perpendicular to the wrinkles, as well as for sliding on a nonwrinkled, flat surface. The mean sliding force for each surface condition is plotted as a function of applied normal load in Fig. 4.

Figure 4 shows that three different coefficients of friction, or constants of proportionality, are required to describe these surfaces, although the interfacial chemistry/composition is identical for each data set. At a normal loading of 60 mN, sliding parallel to the wrinkles, portions of the wrinkled surface are collapsed during sliding; however this change does not appear to change the relation between frictional force and applied normal load.

To demonstrate that the changes in contact area for wrinkled surfaces compared to nonwrinkled surfaces cannot explain the decrease in sliding resistance suggested in Figs. 3 and 4, we normalize the mean sliding force by the measured contact area during sliding (A) to define the sliding shear stress (σ). The sliding shear stress of the wrinkled surfaces sliding parallel and perpendicular to the wrinkle alignment direction normalized by the sliding shear stress of a flat PDMS surface is plotted as a function of aspect ratio (Fig. 5). These results indicate that for both sliding parallel and perpendicular to wrinkles; the sliding resistance decreases relative to a nonwrinkled surface with more pronounced effects observed for greater aspect ratios. This result emphasizes by virtue of the area normalization that wrinkles do not alter the sliding resistance by decreasing the sliding contact area, but rather an alternative mechanism is responsible for decreasing the sliding resistance for wrinkled surfaces.

[This article is copyrighted as indicated in the abstract. Reuse of AIP content is subject to the terms at: http://scitation.aip.org/termsconditions. Downloaded to] IP: 128.119.168.228 On: Mon, 28 Oct 2013 15:50:39

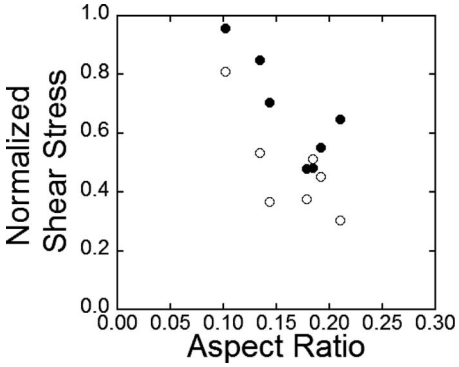

FIG. 5. Normalized shear stress vs wrinkle aspect ratio (●—sliding parallel and ○—sliding perpendicular).

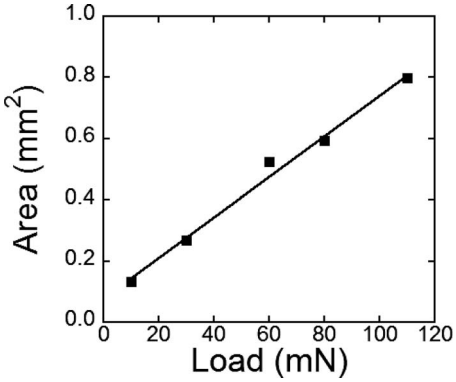

FIG. 6. Sliding contact area vs normal load for the flat surface with a linear fit.

IV. DISCUSSION

To understand the change in frictional force associated with surface wrinkles, we adapt the classical friction model presented by Bowden and Tabor[22] to

$$F = \frac{G_c}{l} A, \tag{1}$$

where F is the frictional force, G_c is the adhesion energy or the critical energy release rate for interfacial fracture at the slider/substrate interface, l is a materials-defined length scale associated with the interfacial fracture process at the slider/substrate interface, and A is the true contact area during sliding. A key assumption for this model is homogeneity and isotropy in the lateral stiffness of the interface. Lateral stiffness k is the defined as the required change in lateral force per change in lateral displacement for a nonsliding interface. For homogenous isotropic materials, $k \propto \mu a$ where μ is the geometric mean of the shear moduli for the slider/substrate materials and a is the contact radius of an interface. For an interface with heterogeneities, such as topographic features, k depends upon additional geometric corrections.[23] As discussed in a previous publication, these changes in lateral stiffness can be accounted for in the Bowden–Tabor model by introducing a nondimensional correction factor f_x defined as the ratio of the lateral stiffness for the topographically patterned surface to the lateral stiffness for a nonpatterned interface of the same materials[23]

$$F \propto \frac{\mathcal{G}_c A f_x^2}{l} \quad \text{or} \quad \sigma \propto \frac{\mathcal{G}_c f_x^2}{l} \tag{2}$$

With this simple model, it is straightforward to understand the primary mechanisms behind the sliding resistance of wrinkled surfaces observed in the results above.

Figure 4 demonstrated that the average sliding force is directly proportional to the applied normal load for both wrinkled and nonwrinkled surfaces. Although Hertzian contact mechanics dictates that $A \propto P^{2/3}$ for nonsliding interfaces, we measure $A \propto P$ during sliding (Fig. 6). Therefore, the relationship in Eq. (2) supports the linear scaling between frictional force and normal load in Fig. 4 and indicates that the tangential stiffness correction factor f_x and $\mathcal{G}_c$ are primarily responsible for the different coefficients of friction measured for each surface in Fig. 4.

The correction factor f_x is directly measured from the initial slope of the lateral force versus displacement data prior to the initiation of sliding. As shown in the representative data in Fig. 3, the initial slope for both wrinkled surfaces is nearly equal, and both are significantly less than the initial slope for the nonwrinkled surface. Accounting for the true contact area for both wrinkled and nonwrinkled surfaces, we measure $f_x \sim 0.7$ for all wrinkled samples, independent of sliding direction. According to the simple model for friction presented above, this change in the lateral stiffness agrees well with the approximate 50% difference between coefficients of friction for wrinkled surfaces compared to flat surfaces. Furthermore, this simple model relating the changes in lateral stiffness associated with micropatterned surfaces to decreased frictional forces is consistent with recent experimental observations by Varenberg and Gorb[24] for hexagonally arranged microposts. This similarity in frictional force control by vastly different patterns, i.e., wrinkles and hexagonally arranged posts, supports the strong role that lateral stiffness plays in defining micropattern friction for soft interfaces.

In addition to the general decrease in sliding resistance for wrinkled surfaces, the sliding resistance is less for sliding perpendicular compared to sliding parallel, both as a function of applied load and wrinkle aspect ratio. This result is nonintuitive but can be explained by considering the process of sliding as a local fracture process at the trailing edge of the sliding interface. In interfacial fracture, it is well established that the opening angle of the fracture front dictates the required $\mathcal{G}_c$ for propagation.[25] The opening angle defines the mode of fracture, with mode I defined for loading normal to the fracture plane and mode II for loading parallel to the fracture plane, or in shear. The critical energy release rate $\mathcal{G}_c$ for facture is different for mode I and mode II, and for opening angles between 0 and $\pi/2$, $\mathcal{G}_c$ is defined by a combination of $\mathcal{G}_c$ for both mode I (normal) and mode II (shear) fracture modes. In practical terms, this effect relates to the change in force required to peel a piece of tape from a rigid surface as a function of the peel angle. For true sliding, the fracture angle at the trailing edge will be approximately 0°, or mode II fracture. For sliding with Schallamach waves, fracture proceeds at angles near $\pi/2$ or mode I, as demonstrated in the work of Koudine and Barquins[26] For wrinkled

[This article is copyrighted as indicated in the abstract. Reuse of AIP content is subject to the terms at: http://scitation.aip.org/termsconditions. Downloaded to] IP: 128.119.168.228 On: Mon, 28 Oct 2013 15:50:39

surfaces presented here, the wrinkles serve as permanent Schallamach waves since the wrinkle periodicities were similar to the Schallamach wave periodicities measured in the flat sample. Therefore, we hypothesize that the surface wrinkles serve the same role as Schallamach waves in altering, i.e., lowering, the $\mathcal{G}_c$ for lateral displacement of the interface by causing sliding to occur in a mode I mechanism. For sliding parallel to the wrinkles, Schallamach waves were not observed and motion proceeded by true sliding, or mode II fracture. Since $\mathcal{G}_c$ for mode I is commonly less than $\mathcal{G}_c$ for mode II our hypothesis supports the observation that sliding perpendicular to the wrinkle alignment direction requires less force compared to sliding parallel.

V. CONCLUSION

We have shown that surface wrinkles can reduce the sliding frictional force of a sliding hemispherical lens. Three coefficients of friction are required to describe sliding parallel, perpendicular, and on a flat surface, even though these interfaces are comprised of identical materials. The changes in frictional force associated with the wrinkled surfaces are not described by changes in contact area, and nonintuitively the sliding resistance is less for sliding perpendicular to the wrinkle alignment direction. These changes in sliding friction are associated with changes in tangential stiffness and interfacial fracture angle, or fracture mode. In general, these control factors should apply to both anisotropic and isotropic surfaces, as well as other topographic surfaces, thus providing fundamental guidance in the design of surfaces with predictable frictional properties.

ACKNOWLEDGMENTS

This work is supported by the National Scientific Foundation—Material Research Science & Engineering Center on polymers at The University of Massachusetts Amherst, Grant No. DMR-0820506. The authors wish to thank Edwin Chan for his helpful discussions on wrinkled surfaces.

[1]B. Aksak, M. P. Murphy, and M. Sitti, Langmuir **23**, 3322 (2007).
[2]L. Ge, S. Sethi, L. Ci, P. M. Ajayan, and A. Dhinojwala, Proc. Natl. Acad. Sci. U.S.A. **104**, 10792 (2007).
[3]A. K. Geim, S. V. Dubonos, I. V. Grigorieva, K. S. Novoselov, A. A. Zhukov, and S. Y. Shapoval, Nature Mater. **2**, 461 (2003).
[4]N. J. Glassmaker, A. Jagota, C. Y. Hui, and J. Kim, J. R. Soc., Interface **1**, 23 (2004).
[5]S. Gorb, M. Varenberg, A. Peressadko, and J. Tuma, J. R. Soc., Interface **4**, 271 (2007).
[6]C. Greiner, A. del Campo, and E. Arzt, Langmuir **23**, 3495 (2007).
[7]S. Kim and M. Sitti, Appl. Phys. Lett. **121905**, 89 (2006).
[8]M. Sitti and R. S. Fearing, J. Adhes. Sci. Technol. **17**, 1055 (2003).
[9]M. Varenberg and S. Gorb, J. R. Soc., Interface **4**, 721 (2007).
[10]C. Majidi, R. E. Groff, Y. Maeno, B. Schubert, S. Baek, B. Bush, R. Maboudian, N. Gravish, M. Wilkinson, K. Autumn, and R. S. Fearing, Phys. Rev. Lett. **97**, 076103 (2006).
[11]E. P. Chan, E. J. Smith, R. C. Hayward, and A. J. Crosby, Adv. Mater. **20**, 711 (2008).
[12]A. Schallamach, Wear **17**, 301 (1971).
[13]M. Ouyang, C. Yuan, R. J. Muisener, A. Boulares, and J. T. Koberstein, Chem. Mater. **12**, 1591 (2000).
[14]K. Efimenko, W. E. Wallace, and J. Genzer, J. Colloid Interface Sci. **254**, 306 (2002).
[15]C. L. Mirley and J. T. Koberstein, Langmuir **11**, 1049 (1995).
[16]K. Efimenko, M. Rackaitis, E. Manias, A. Vaziri, L. Mahadevan, and J. Genzer, Nature Mater. **4**, 293 (2005).
[17]E. Cerda and L. Mahadevan, Phys. Rev. Lett. **90**, 074302 (2003).
[18]C. J. Rand and A. J. Crosby, Appl. Phys. Lett. **89**, 261907 (2006).
[19]M. Barquins, Mater. Sci. Eng. **73**, 45 (1985).
[20]K. L. Johnson, *Contact Mechanics*, 9th ed. (Cambridge University Press, Cambridge, U.K., 2003).
[21]K. L. Johnson, J. A. Greenwood, and J. G. Higginson, Int. J. Mech. Sci. **27**, 383 (1985).
[22]F. P. Bowden and D. Tabor, *The Friction and Lubrication of Solids* (Clarendon, Oxford, 1964).
[23]C. J. Rand and A. J. Crosby, Appl. Phys. Lett. **91**, 261909 (2007).
[24]M. Varenberg and S. N. Gorb, Adv. Mater. **21**, 483 (2009).
[25]D. H. Kaelble, Trans. Soc. Rheol. **3**, 161 (1959).
[26]A. A. Koudine and M. Barquins, J. Adhes. Sci. Technol. **10**, 951 (1996).

[This article is copyrighted as indicated in the abstract. Reuse of AIP content is subject to the terms at: http://scitation.aip.org/termsconditions. Downloaded to] IP: 128.119.168.228 On: Mon, 28 Oct 2013 15:50:39